

## SOME CHARACTERISTICS OF TOTAL AND COMPOSITE (AERONOMICAL) MODELS OF PLANETARY ATMOSPHERES

STEVO ŠEGAN and BRANKICA ŠURLAN

*Department of Astronomy, Faculty of Mathematics, University of Belgrade  
Studentski trg 16, 11000 Belgrade, Serbia and Montenegro*

*E-mail: sseگان@matf.bg.ac.yu*

*E-mail: brankica74@matf.bg.ac.yu*

**Abstract.** The most recent atmosphere models usable in the theory of Earth Artificial Satellites (EAS) motion are analysed. The advantage of the so-called total-density models in the cases of application to the calculation of perturbations in the EAS motion caused by the atmosphere drag is indicated. The parameters of our own model obtained for the perigee distances of 100-800 km are given.

### 1. INTRODUCTION

Most satellite orbits contract slowly under the influence of air drag. The drag depends on the density of the upper atmosphere, which varies widely and irregularly, and depends in particular on the future variations of solar activity, which are at present unpredictable in detail. Some of more than few thousand satellites in orbit now being tracked, and these are decaying in the rate of about 10 per week. To know how many fragments may reach the ground is particularly connected with the knowing of the atmospheric density at perigee height.

In this paper we examine densities derived from aeronomic atmospheric models based on accelerometer measurements in a low Earth's orbit (LEO) and compare the measured densities with those predicted by different empirical models.

### 2. SATELLITE DRAG AND DENSITY VARIABILITY

The procedure for predicting decay is first to assume that the air density will remain constant during the rest of the life of the satellite and to calculate, either from theory or by numerical integration, the date at which the perigee will descend below 100 km. The rate of decay of orbital period is mainly used as a measure of the air drag.

We know that in practice air density always changes and estimating it from some orbital parameters changes is about  $\pm 10\%$  as the best that can consistently be achieved. Occasional good luck will give apparently more accurate results.

As in the previous paper (Šegan, 1988; Šegan, Pejović, 1992, 1993) we start from the equation of hydrostatic equilibrium

$$\frac{dp}{dr} = -\frac{\mu}{r^2}MN = -g(r)\rho \quad (1),$$

where the Earth's parameter  $\mu = 398601.3 \text{ km}^3/\text{s}^2$ ,  $M$  is the mean molecular mass of the air,  $N$  is the number of molecules,  $\rho$  is the air density and  $r$  is the geocentric distance, assuming  $\Delta r \ll r$  and  $g(r) = \text{const}$  ( $\Delta r$  - height of the atmospheric layer;  $g(r)$  - gravitational acceleration). Then, for ideal gas

$$P = NkT = \rho RT, \quad (2)$$

where  $R = k/M$  is the Earth's atmosphere constant, from (1) we have

$$\frac{dp}{p} = -\frac{\mu M}{kT} \frac{dr}{r^2} = -\frac{gM}{k/T} dh = -\frac{dh}{H} \quad (3)$$

where  $h$  is the altitude and  $H$  scale height. Via the barometric equation

$$p(h) = p(h_0)e^{-(h-h_0)/H}$$

we can calculate the total number of particles (molecules, atoms) by

$$N(r) = \int_r^\infty N(r)dr = \int_0^{p(r)} \frac{r^2}{\mu/M} dp = N(r)H \quad (4)$$

If the atmosphere is oblate following the Earth's spheroid ( $\varepsilon$  - flattening factor), for an arbitrary concentric stratum we have expressions

$$r_{p_0} = R_E^{p_0} (1 - \varepsilon \sin^2 \varphi_{p_0})$$

$$R = r_{p_0} (1 + \varepsilon \sin^2 \varphi_{p_0})(1 - \varepsilon \sin^2 \varphi),$$

where  $R_E$  is the equatorial radius of a given spheroid,  $R$  is the geocentric distance for an arbitrary point of the spheroid, so that at a geocentric distance  $r$  and latitude  $\varphi$  the density is

$$\rho = \rho_{p_0} e^{-(r-R)/H}. \quad (5)$$

During geomagnetically disturbed intervals, atmospheric densities increase due to deposition of energy by energetic particles precipitating from the magnetosphere and by ohmic heating of ionospheric currents driven by ionosphere-magnetosphere coupling. Assuming knowledge of the drag coefficient, area-to-mass ratio and speed of the satellite, the atmospheric density can be determined.

For many years a variety of satellites have flown accelerometers to measure thermospheric density, as well as neutral and ion mass spectrometers to measure the number densities of neutral and ionized composition of the upper atmosphere. In addition, thermospheric densities have also been inferred from the tracking of satellites and

careful analysis of orbital parameter changes with time. All of these data sets have led to the development of thermospheric density, composition and temperature models which are used for orbital prediction studies as well as a number of scientific purposes. The "Mass Spectrometer Incoherent Scatter Extension XXXX" (CIRAAyy, MSISEyy), where "XXXX" can be changed with "1972", "1986", "1990" for successively models and one of the more recent of these models is MSISE90.

### 3. OVERVIEW OF ATMOSPHERE MODELS

Early models of the thermosphere emerged about 1965 (e.g. Harris-Priester, Jacchia-65). These, as well as their descendants (Jacchia, 1971), CIRA-72, and (Jacchia, 1977), were based on a numerical quadrature of the species-wise diffusion equations. In these models the altitude profiles of the number densities  $n_i$  are largely determined by the magnitude of the exospheric temperature  $T_\infty$ . This quantity is used to accommodate all activity concerning the diurnal effects, while semi-annual variations are introduced via empirical correction functions. In the Jacchia-77 model species-wise corrections are also introduced for the diurnal, seasonal/latitudinal, and geomagnetic effects. The numerical integration can be very CPU demanding in orbit predictions. In order to improve the time dependence for calls to such routines, (Mueller, 1982) implemented the Jacchia-Lineberry algorithm for the (Jacchia, 1971) model, and (Lafontaine and Hughes, 1983) developed an equally efficient method to approximate the Jacchia-77 model. The MET-87 model (Marshall Engineering Thermosphere Model, Hickey, 1988) is also based on the early Jacchia-71 atmosphere, but it extends the range of output quantities, including the pressure, the pressure scale height and the ratio of specific heats.

Another line of atmosphere models directly applies analytical solutions of the simplified diffusion equations to derive concentration profiles. The most prominent class of these models is called MSIS (Mass Spectrometer and Incoherent Scatter, Hedin 1987, 1991, 1991).

The MSIS models were continuously improved in 1977, 1983, and 1986 on the basis of new measurement data so that new results became available. MSIS-86 also became the reference atmosphere model referred to as CIRA-86 for thermospheric altitudes. Recently, MSIS-86 was upgraded to MSISE-90 by a continuation to ground level with smooth density and temperature profiles. The DTM-77 model (Density and Temperature Model) by Barlier et al. (1977) has a similar structure as MSIS-77 but it limits itself to the constituents N<sub>2</sub>, O<sub>2</sub>, O, and He (Barlier et al., 1977; Koehnlein, 1979). Hydrogen, which becomes dominant at high altitudes especially for low activity levels, is not taken into account. The C model by Proelss et al. (1985) also has a MSIS-77 structure with modified correction functions. The advantage of MSIS, DTM, and C lies in their model flexibility to account for observed changes, and in their comprehensive range of output results (including number densities).

In these models, for simplicity we have assumed

$$T(z) = T_\infty - (T_\infty - T_{120})e^{-\sigma z}$$

where  $T_\infty$  is the temperature in the thermopause,  $T_{120}$  is the temperature at the 120

km boundary and

$$\zeta = (z - 120)(R + 120)/(R + z), \quad R = 6356.77 \text{ km},$$

is the geopotential height, whereas  $\sigma$  is connected with the temperature-gradient parameter  $s$  ( $s \approx 0.02$ ) via

$$\sigma = s + (R + 120)^{-1}.$$

The different constituent concentration will be expressed through the spherical functions (Hedin, 1986; Barlier, 1978). Explicitly, the number densities are

$$n_i(z) = A_i e^{(G_i(L)-1)f_i(z)}$$

where is (Walker, 1965; Bates, 1959)

$$f_i(z) = ((1 - a)/(1 - ae^{\sigma\zeta})^{1+\alpha_i+\gamma_i} e^{-\sigma\gamma_i\zeta}$$

and

$$a = (T_\infty - T_{120})/T_\infty, \quad \gamma_i = (m_i g_{120})/(\sigma k T_\infty)$$

where  $m_i$  is the molecular mass,  $k$  is Boltzmann's constant,  $g_{120}$  gravitational acceleration at 120 km height; the functions  $G_i(L)$  are dependent of the physical parameters and their expression via the spherical functions is

$$G_i(L) = 1 + f_i(F, \bar{F}, K_p) + \beta \left[ \sum_{p=1}^{\infty} f_2(p, \Omega, d) + \sum_{n=1}^{\infty} \sum_{m=1}^n C_n^m f_3(n, m, \omega, t) \right]. \quad (6)$$

If the perigee height is greater than about 500 km, the orbital lifetime is usually 20 years and more. But most satellites (of our interest) have perigee height between 200 and 500 km, with possible extremely shorter life time (from few days to several months) depending on the exact orbit and the area/mass ratio of the satellite. That mean, the wide variations in air density are indicated for heights between 100 and 1000 km. In predicting orbital lifetime important role has the third class of the atmospheric density models.

A third class of thermosphere models only aims at total densities as an output result. The underlying data of the Russian GOST-84 model are solely derived from the satellite drag analysis. The total density is computed from a reference altitude profile which is adjusted with four factors accounting for (1) diurnal, (2) seasonal/latitudinal, (3) solar activity, and (4) geomagnetic activity effects. An updated set of model coefficients was published in 1990. The TD-88 model (Sehnal et al., 1988) is more flexible in its formulation since TD-88 does not assume a rigorous separation of perturbing effects (factorization of corrections) as done in GOST-84. The TD-88 model, however, should be applied only at altitudes from 150 km to 750 km.

The variation in density at given height when the solar activity changes from sunspot maximum to sunspot minimum is important for these studies: at a height of 500 km the density is about 10 times greater at sunspot maximum than at sunspot minimum! So, a satellite in a circular orbit at a height of 500 km might have lifetime of 5 years if launched a little before solar minimum, but a lifetime of 6 months if launched at solar maximum.

The figures also shows that there is a large variation in density between day and night: the density being much greater by day than by night, by factor of up to about 5 at same height.

#### 4. THE COMPARISON OF THE MODELS

In applications which require a smooth, continuous density profile with altitude the 'deviation from the diffusive equilibrium' option in MSISE-90 (MSISE-00) should be switched off (corresponding to switch setting  $SW(15) = 0.0$ ).

The MSISE-90 Model will be compared with others with special attention given to the TD-88 model.

We have exploited a partially changed original routine (Hedin, 1991) which is designed to give us the MSIS total mass density values evaluated at a given local time and latitude location over a course of day and annual season. For a sun-synchronous orbit the local time is fixed, but the longitude changes as the Earth rotates. The input parameters necessary to obtain the MSISE-90(00) density values are the following:

Input Year and Day of Year	YD
Time step in hours	LTh
Altitude in km	ATh
Latitude in degrees	$\varphi$
Local Time in hours	LT
F10.7 cm (2800MHz) Solar Flux Values	F
Three-Month Average of F10.7	$\overline{F}$
Daily $K_p$ Indices	$K_p$

We have prepared a series of plots to make a number of comparisons.

For each of the following comparisons, we have made comments on the behavior of the measured and modelled atmospheric densities, indicating the plots by number. For the purpose of comparing the two most interesting models - TD-88 and MSISE-00 - we present Figs. 1 – Fig. 21.

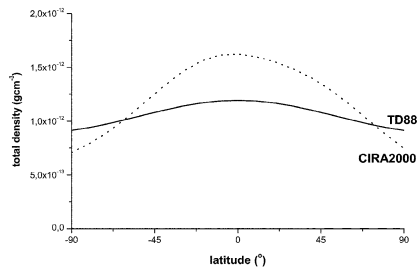


Figure 1: Dependence of the total density on latitude obtained by using TD-88 and MSISE-00; YD=80, LTh=24, ATh=500,  $\varphi=(-90-90)$ , LT=14, F=150,  $\overline{F}=150$ , Kp=3.

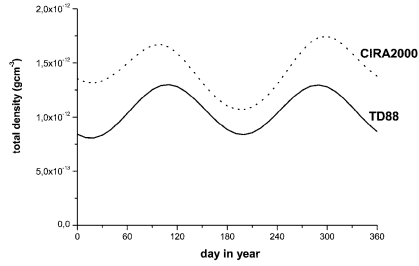


Figure 2: Dependence of the total density on the day in the year obtained by using TD-88 and MSISE-00; YD=(0-360), LTh=24, ATh=500,  $\varphi=0$ , LT=14, F=150,  $\overline{F}=150$ , Kp=3.

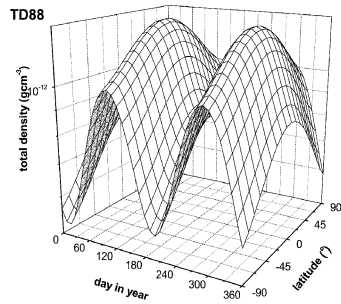


Figure 3: Dependence of the total density on the day in year and on the latitude obtained by using TD88.

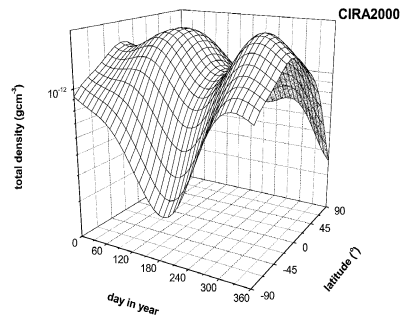


Figure 4: Dependence of the total density on the day in year and on the latitude obtained by using MSISE-00.

YD=(0,360), LTh=24, ATh=500,  $\varphi=(-90-90)$ , LT=14, F=150,  $\overline{F}=150$ , Kp=3, for Fig. 3 and 4.

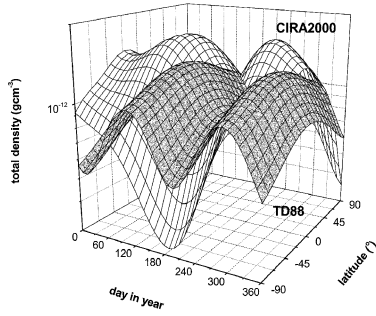


Figure 5: Comparison of the dependence of the total density on the day in year and on the latitude obtained by using TD88 and MSISe-00; YD=(0-360), LTh=24, ATh=500,  $\varphi=(-90-90)$ , LT=14, F=150,  $\bar{F}=150$ , Kp=3.

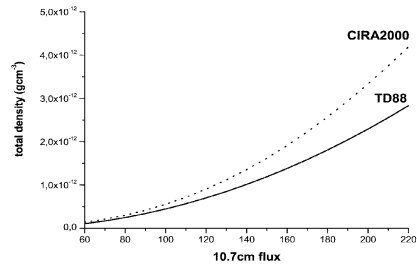


Figure 6: Dependence of the total density on flux obtained by using TD-88 and MSISe-00; YD=80, LTh=24, ATh=500,  $\varphi=0$ , LT=14, F=(60-220),  $\bar{F}=(60-220)$ , Kp=3.

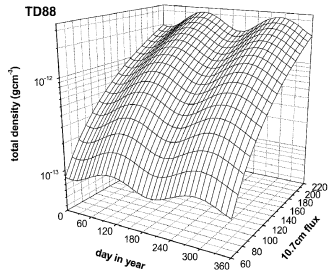


Figure 7: Dependence of the total density on the day in the year and on the flux obtained by using TD88.

YD=(0-360), LTh=24, ATh=500,  $\varphi=0$ , LT=14, F=(60-220),  $\bar{F}=(60-220)$ , Kp=3, for Fig. 7 and 8.

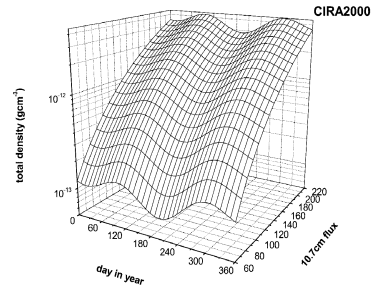


Figure 8: Dependence of the total density on the day of the year and on the flux obtained by using MSISe-00

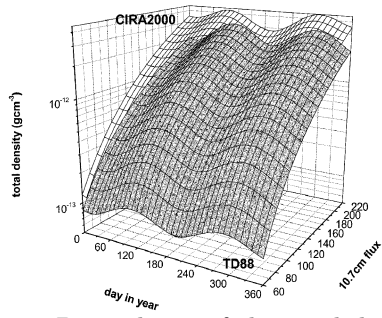


Figure 9: Dependence of the total density on the day in the year and on the flux obtained by using TD88 and MSISe-00;  $YD=(0-360)$ ,  $LTh=24$ ,  $ATh=500$ ,  $\varphi=0$ ,  $LT=14$ ,  $F=(60-220)$ ,  $\bar{F}=(60-220)$ ,  $Kp=3$ .

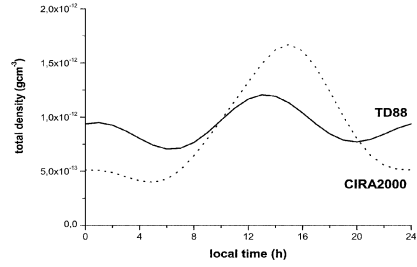


Figure 10: Dependence of the total density on local time obtained by using TD88 and MSISe-00;  $YD=80$ ,  $LTh=24$ ,  $ATh=500$ ,  $\varphi=0$ ,  $LT=(0-24)$ ,  $F=150$ ,  $\bar{F}=150$ ,  $Kp=3$ .

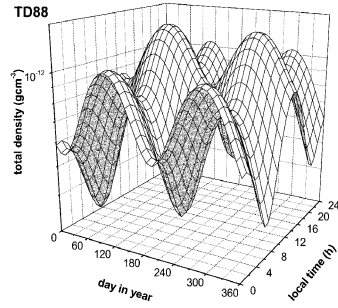


Figure 11: Dependence of the total density on the day in the year and on the local time obtained by using TD88.

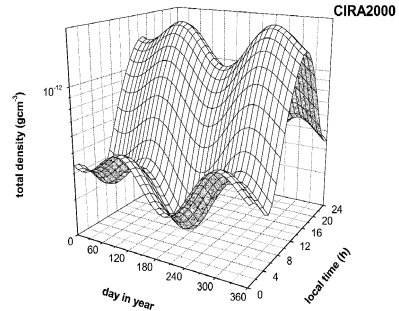


Figure 12: Dependence of the total density on the day in the year and on the local time obtained by using MSISe-00

$YD=(0-360)$ ,  $LTh=24$ ,  $ATh=500$ ,  $\varphi=0$ ,  $LT=(0-24)$ ,  $F=150$ ,  $\bar{F}=150$ ,  $Kp=3$ , for Fig. 11 and 12.



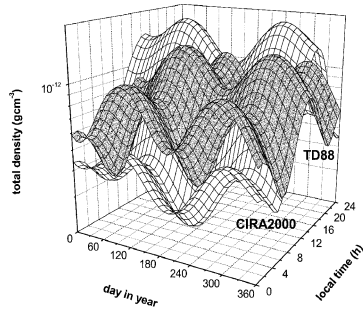


Figure 13: Dependence of the total density on the day in the year and on the local time obtained by using TD88 and MSISe-00;  $YD=(0-360)$ ,  $LTh=24$ ,  $ATh=500$ ,  $\varphi=0$ ,  $LT=(0-24)$ ,  $F=150$ ,  $\bar{F}=150$ ,  $Kp=3$ .

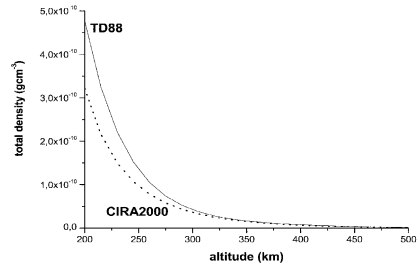


Figure 14: Dependence of the total density on altitude obtained by using TD88 and MSISe-00;  $YD=80$ ,  $LTh=24$ ,  $ATh=(200-500)$ ,  $\varphi=0$ ,  $LT=14$ ,  $F=150$ ,  $\bar{F}=150$ ,  $Kp=3$ .

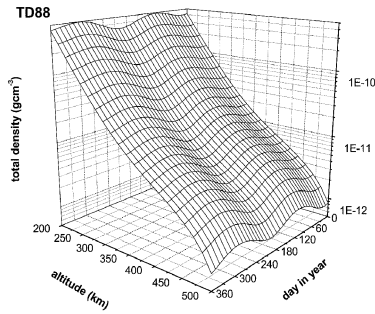


Figure 15: Dependence of the total density on the day in the year and on the altitude obtained by using TD88.

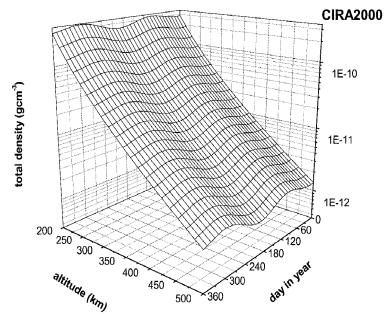


Figure 16: Dependence of the total density on the day in the year and on the altitude obtained by using MSISe-00

$YD=(0-360)$ ,  $LTh=24$ ,  $ATh=(200-500)$ ,  $\varphi=0$ ,  $LT=14$ ,  $F=150$ ,  $\bar{F}=150$ ,  $Kp=3$ , for Fig. 15 and 16.

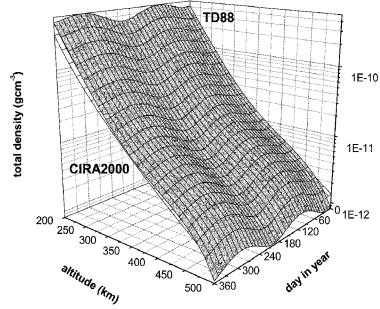


Figure 17: Dependence of the total density on the day in the year and on the altitude obtained by using TD88 and MSISe-00; YD=(0-360), LTh=24, ATh=(200-500),  $\varphi=0$ , LT=14, F=150,  $\bar{F}=150$ , Kp=3.

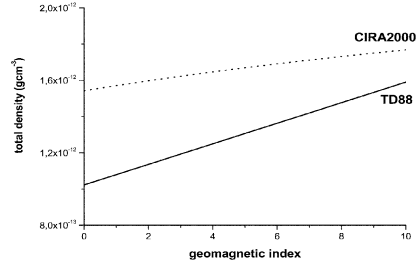


Figure 18: Dependence of the total density on geomagnetic index obtained by using TD-88 and MSISe-00; YD=80, LTh=24, ATh=500,  $\varphi=0$ , LT=14, F=150,  $\bar{F}=150$ , Kp=(0-10).

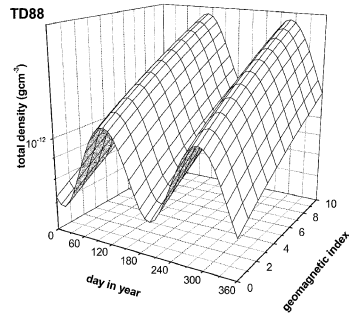


Figure 19: Dependence of the total density on the day in the year and on the geomagnetic index obtained by using TD88.

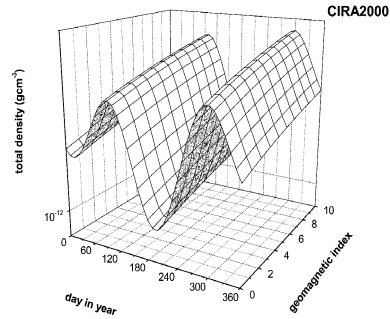


Figure 20: Dependence of the total density on the day in the year and on the geomagnetic index obtained by using MSISe-00

YD=(0-360), LTh=24, ATh=4500,  $\varphi=0$ , LT=14, F=150,  $\bar{F}=150$ , Kp=(0-10), for Fig. 19 and 20.

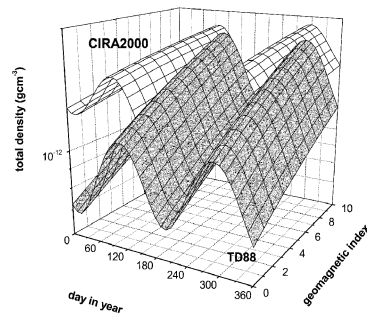


Figure 21: Dependence of the total density on the day in the year and on the geomagnetic index obtained by using TD88 and MSISe-00; YD=(0-360), LTh=24, ATh=500,  $\varphi=0$ , LT=14, F=150,  $\bar{F}=150$ , Kp=(0-10).

The unpredictability of solar activity is the main difficulty in predicting lifetimes of the order of several years or a few days! With lifetimes of intermediate length, between one month and year, another partially unpredictable variation becomes most important: this is semi-annual variation in density. Under constant conditions (fixed height, effects of solar activity removed, smoothed daily irregularities, etc...) there is an oscillation approximately every 6 months: the density changes by a factor 1.7 so lifetime prediction can be in error by up to 30% if no allowance is made for the semi-annual variation.

## 5. CONCLUSIONS

Two models of the Earth's upper atmosphere are presented theoretically and graphically. The variation of the density with the inclusion of the effects of solar activity and of the semi-annual effect is can be calculated only in particular cases.

The MSIS, is a very complex but very precise model. TD-model is very flexible and simply applicable.

## References

- anon.: 1972, "CIRA-72 (COSPAR International Reference Atmosphere 1972)", Akademie Verlag, Berlin.
- anon.: 1984, "Density Model for Satellite Orbit Predictions", GOST 25645-84, Standards Editing House, Moscow.
- Barlier, F., Berger, C., Falin, J.L., Kocharts, G. and Thuiller, G.: 1977, "A Thermospheric Model Based on Satellite Drag Data", *Aeronomica Acta A*, 185.
- Hedin, A.E.: 1987, "MSIS-86 Thermospheric Model", *Journal of Geophysical Research*, **Vol. 92**, **No. A5**, pp. 4649-4662 .
- Hedin, A.E.: 1991, "Extension of the MSIS Thermosphere Model into the Middle and Lower Atmosphere", *Journal of Geophysical Research*, **Vol. 96**, **No. A2**, pp. 1159-1172.
- Hedin, A.E.: 1991, "Revised Global Model of Thermosphere Winds Using Satellite and Ground-Based Observations", *Journal of Geophysical Research*, **Vol. 96**, **No. A5**, pp. 7657-7688.
- Hickey, M.P.: 1988, "The NASA Marshall Engineering Thermospheric Model", *NASA CR-179359*.
- Jacchia, L.G.: 1971, "Revised Static Models of the Thermosphere and Exosphere with Empirical Temperature Profiles", *SAO Report*, **332**, May 5.
- Jacchia, L.G.: 1977, "Thermospheric Temperature, Density, and Composition - New Models", *SAO Report*, **375**, March 15.

- Koehnlein, W. et al.: 1979, "A Thermospheric Model of the Annual Variations of He, N, O, N<sub>2</sub> and Ar from AEROS Nims Data", *Geophys. Res.*, **84**, pp. 4355-4362.
- Lafontaine, J.; Hughes, P.: 1983, "An Analytic Version of Jacchia's 1977 Model Atmosphere", *Celestial Mechanics*, **29**, 3-26.
- Mueller, A.: 1982, "Jacchia-Lineberry Upper Atmosphere Density Model", *NASA Report*, **82-FM-52/JSC-18507**, Oct.
- Proelss, G.W. and Blum, P.W.: 1985, "Comparison of Recent Empirical Models of the Thermosphere", *Proceedings of ESA workshop on Re-Entry of Space Debris, Darmstadt, 24-25 September 1985 (ESA SP-245)*.
- Sehnal, L. and Pospíšilova, L.: 1988, "Thermospheric Model TD 88", *Preprint No. 67*, Observatory Ondřejov.
- Šegan, S.: 1988, "Analytical Computation of Atmospheric Drag Effects", *Cel. Mech.*, **41**, 381.
- Šegan, S. and Pejović, N.: 1992, "The Motion of an Artificial Satellite in the Oblate Atmosphere", *Bull. Astron. Belgrade*, **145**, 101.
- Šegan, S. and Pejović, N.: 1993, "Scale Heights for the Aeronomical Models and Perturbations of Satellite Orbits", *Bull. Astron. Belgrade*, **148**, 17.